

FULL PAPER

## TOWARDS A ROUTINE METHODOLOGY FOR ASSESSING THE CONDITION OF HISTORIC SILK

Jeongjin Kim<sup>1\*</sup>, Paul Wyeth<sup>2</sup>

1. Practical Arts Education, Jinju  
National University of Education,  
Kyungnam, 660-756, Korea

2. The Textile Conservation Centre,  
University of Southampton, Winchester  
Campus, Park Avenue, Winchester,  
Hampshire SO23 8DL, UK

corresponding author:  
jin1827@yonsei.ac.kr

**To ensure continued access and long-term preservation it is essential to understand the condition of an artefact, and the behaviour of its component materials, in order to set limits on display and handling. In support of curators and conservators of collections with historic textiles, we are developing rapid and routine technology, involving near infrared spectroscopy coupled with multivariate analysis, which, when applied non-invasively on-site, will allow the estimation of the state of deterioration of silk fabrics. Pursuing this aim, we have now carried out further analytical studies on silks artificially aged under different regimes for up to 20 days: dry thermal, high heat and humidity, and sunlight equivalent irradiation. The tensile strengths, yellowness indices, apparent molecular weights of fibroin, and near infrared spectral sorbed moisture parameters for the aged silks were determined. The mechanical performance of silk diminished exponentially over each ageing time course. For the various silks, the increases in yellowness indices and decreases in fibroin molecular weights and moisture contents showed similar kinetics to the mechanical changes. While each parameter was correlated with the tensile strength, silks exposed to the different accelerated ageing factors exhibited diverse correlations. It is concluded that, when formulating a general model for characterising the condition of silk using chemometrics, the reference set should include examples of silks which have been exposed to the full variety of ageing factors.**

### 1 Introduction

A variety of risks threaten the well being of our tangible heritage. The associated hazards include environmental exposure and handling, for example. For curators and conservators, an appreciation of the condition of artefacts is fundamental to mitigating such risks in relation to display or treatment. Our research is directed at an understanding of historic silks. Besides investigating the deterioration of silks, we are also keen to establish routine instrumental analytical methodology for

received: 07.04.2009  
accepted: 15.06.2009

key words:  
Silk, fibroin, accelerated ageing, condition, yellowness index, molecular weight, sorbed moisture

characterising the current physical condition of fabrics in collections.

Previously we have estimated the silk fibroin crystallite orientation by polarized FTIR spectroscopy and determined the apparent acid content of silk by microextraction, and, for a series of artificially aged specimens, noted correlations with tenacity for both parameters.<sup>1,2</sup> In similar studies, others have considered the molecular weight of silk fibroin<sup>3</sup> and the amino acid content of urea extracts of silk<sup>4</sup> as potential markers of condition. However, the requirement for sampling, and other constraints, means that none of the associated techniques could be used routinely for assessing historic silks. We are therefore investigating the potential of other methodology, especially non-invasive procedures such as near infrared spectroscopy (NIR) coupled with multivariate analysis.<sup>5</sup> In this case models are generated from reference data, which allow the correlation of spectral patterns with mechanical performance, providing a means of deducing the condition of historic specimens indirectly.

In developing the predictive models for this approach, a better understanding of the ageing behaviour of silk is required. For historic silks the complete biographical details of environmental exposure are seldom known. The range of possible promotional ageing factors (heat, light etc) may elicit differential effects. In that case, when model building, it is essential to include in the reference set silks that are known to have been aged by these various factors.

In this paper we report further analytical studies on artificially aged silks which show that light, heat and humidity accelerated ageing can produce different condition-related correlations, contrary to the results from our earlier polarized FTIR and pH studies. This time the silks were subjected to colour measurements, molecular weight estimations by high performance size exclusion chromatography (HPSEC), and NIR sorbed moisture determinations. This has implications for the chemometric approach to non-invasive condition assessment.

## 2 Experimental

### 2.1 Silk

Undyed, plain-weave silk fabric (Whaleys habotai silk, 40 gm<sup>-2</sup>; thread count per cm: warp 147, weft 122) was degummed in a 1% sodium dodecylsulfate + 1% sodium carbonate solution for 1 h at 98±2 °C, rinsed thoroughly in purified water and dried at

room temperature. The fabric was then cut into 25 mm wide strips along the warp for artificial ageing.

### 2.2 Artificial Ageing

Accelerated ageing conditions were selected to degrade the test fabric to a range of strengths after reasonable exposure times, and to reflect variations in the conditions to which silks can be exposed. Silk specimens were separately subjected to dry thermal ageing (125 °C) in air, high temperature and humidity ageing in a closed chamber (100 °C, 100% RH) in air or under nitrogen (O<sub>2</sub> < 0.1%) , and sunlight equivalent ageing (25 MJ/m<sup>2</sup> over one day) in air, for periods up to 20 days. Details of the ageing protocol have already been reported.<sup>2</sup>

### 2.3 Tensile Tests

Fabric strips, measuring 2.5×5 cm, were conditioned for at least 72 h at 20±2 °C, 55±5% RH. Data were then acquired under the same ambient conditions on an Instron 5544 instrument, adapting the standard method for fabric strips BS EN ISO 13934-1:1999, with gauge lengths of 3.0 cm and a crosshead speed of 2 mm/min. Six replicates from each sample were analyzed, discarding the results for strips which broke close to the jaws and calculating average values for the remainder; there were four or more valid replicates in each case. The tensile strength was taken as the load (N) at break.

### 2.4 Colour Measurement

Colour was measured using the CIELAB colour system, with a Minolta CR-210 Chromameter, a C illuminant and 2° observation; the silk samples were placed on the white reference for measurement. The CIE L\*, a\* and b\* colour coordinates were recorded for six replicate measurements, the X, Y and Z tristimulus values were calculated and, in turn, the average yellowness indices of the samples according to ASTM E313.

### 2.5 High Performance Size Exclusion Chromatography

The methodology for HPSEC was adapted from that developed for silk analysis by Hallett and Howell.<sup>3,6</sup> Due to resource constraints just the specimens artificially aged in air were studied. For each sample, 1.6 mg of fabric was dissolved in 0.25 ml concentrated aqueous lithium thiocyanate (1.4 g/ml). The solution, in a capped polypropylene-

ne tube, was allowed to stand overnight at room temperature and then filtered by centrifugation (Eppendorf Minispin) through a 0.45  $\mu\text{m}$  Millipore filter, although there was no visible residue in any case. HPSEC was carried out on a Thermo-Finnigan system with a Phenomenex 'BIOSEP-SEC-S 4000' column (300x4.6 mm), maintained at 30 °C. 20  $\mu\text{l}$  of a silk solution was injected into the system and elution performed with 8 M urea + 0.05 M tris(hydroxymethyl)aminomethane hydrochloride buffer (pH 7) at 0.5 ml/min. Eluate absorbance readings were taken at 280 nm. The data were recorded and processed with EZChrom software.

Blue dextran (Mw 2000 kDa) was used as a marker of the void volume of the column, while the thiocyanate peak gave an indication of the additional internal volume. The system was calibrated with protein molecular weight standards from Sigma: bovine carbonic anhydrase (29 kDa), bovine serum albumin (66 kDa), yeast alcohol dehydrogenase (150 kDa), and sweet potato  $\beta$ -amylase (200 kDa). For the silks, the weight-averaged molecular weights,  $M_w$ , were calculated with the EZChrom software, considering 0.5 min slices over the analysed portion of the trace:

$$M_w = \frac{\sum A_t \cdot M_t}{\sum A_t}$$

where  $A_t$  is the area of a peak slice, and  $M_t$  the calibration mass for that slice.

The results presented are the means of triplicate analyses. The values of the molecular weight are nominal since, although run under denaturing conditions, the conformations of the proteins and hence their hydrodynamic radii are uncertain (eg when hydrophobic moieties aggregate). Furthermore, the above equation for  $M_w$  is exact only if it is assumed that the mass extinction coefficient is invariant for the silk fragments, which may not be the case.

## 2.6 NIR Spectroscopy – Sorbed Moisture

Reflectance NIR spectra were acquired using a Perkin Elmer Spectrum One NTS spectrometer equipped with an Axiom fibre optic probe, over the range 10,000-4,000  $\text{cm}^{-1}$ , at a resolution of 8  $\text{cm}^{-1}$ , and for 256 scans. Spectralon was used as the reference. Each single layer silk sample was laid over a hole on a card support. The probe window was placed parallel and immediately adjacent to the silk sample, below the hole and without contact, with consistent alignment of the fabric. Spectra were recorded at five different positions on each sample (under ambient conditions of 20 $\pm$ 2 °C and RH 50 $\pm$ 2%), and subsequently manipulated

with Thermo Galactic GRAMS/32 AI software. Spectral sorbed moisture parameters reflecting the relative moisture contents were determined according to protocol developed previously,<sup>8</sup> with slight modification. For each spectrum the intensity of the O-H combination band at 5170  $\text{cm}^{-1}$  was measured following Kubelka Munk correction, generation of the second derivative with the Gap function and subsequent normalization (to a methylene band at 5944  $\text{cm}^{-1}$ ).

## 3 Results and Discussion

### 3.1 Tensile Strengths of Aged Silks

As reported previously, progressive degradation of silk results in an exponential loss of strength (Figure 1). Placing silk under nitrogen seems to have little consequence on the decrease in tenacity effected by high temperature and humidity, suggesting that, under similar conditions in air, hydrolysis rather than oxidative deterioration is dominant. The curves on the plot are exponential regression fits, generated using MS Excel, with coefficients of determination ( $R^2$ ) 0.99, 0.91 and 0.99 (top to bottom); since for a perfect fit  $R^2 = 1$ , the exponential model seems to be good for all cases. The associated first order decay constants are 0.06 $\pm$ 0.01, 0.14 $\pm$ 0.02 and 0.25 $\pm$ 0.02  $\text{day}^{-1}$  for dry thermal, high temperature and humidity (combined data), and sunlight equivalent ageing, respectively.

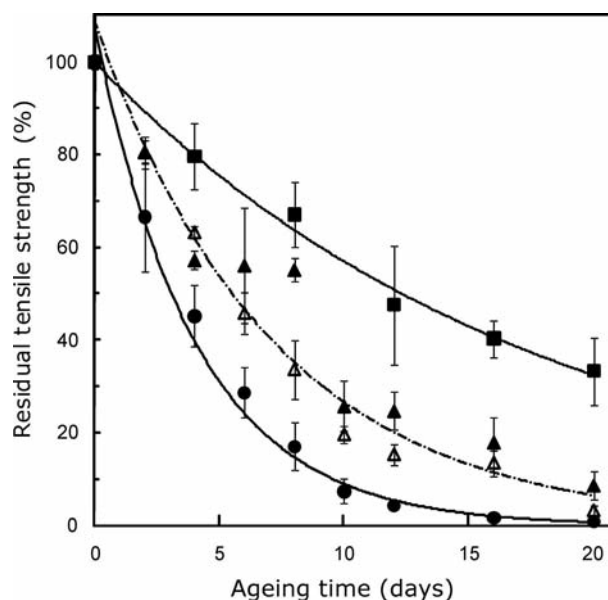


Figure 1. Plots of the percentage residual tensile strengths of the silk samples versus ageing time, for dry thermal ageing (■), high temperature and humidity ageing (▲), anoxic high temperature and humidity ageing (▼), and sunlight equivalent ageing (●). The data points represent the averages for up to six replicates (error bars show the standard deviations). Exponential trend lines were generated using MS Excel.

### 3.2 Colour Measurement

The white silk discoloured upon ageing, becoming pale lemon-yellow with sunlight equivalent exposure, but assuming a darker yellow-brown hue following both dry thermal and raised heat and humidity treatments. The difference is apparent in the plot of the yellowness indices (YI) of the specimens versus ageing time (Figure 2).

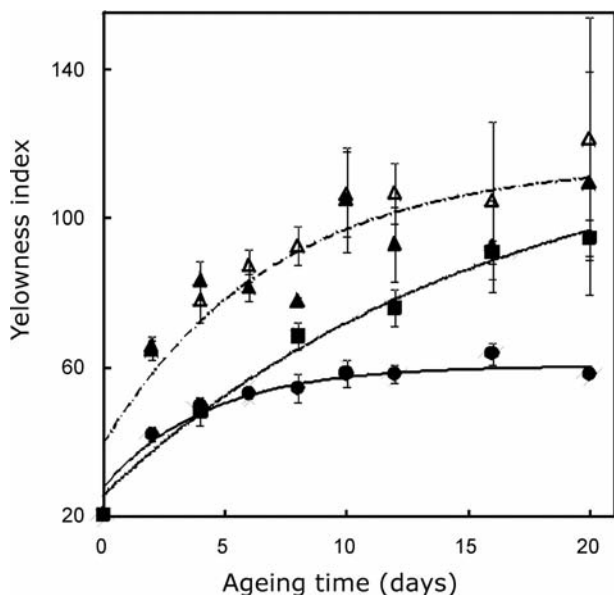


Figure 2. The time course for the change in the yellowness index of silk for each ageing regime (symbols and line styles as for Figure 1); bars show the standard experimental errors. The curves are best fits to the data, using the first order rates determined from the tensile test results.

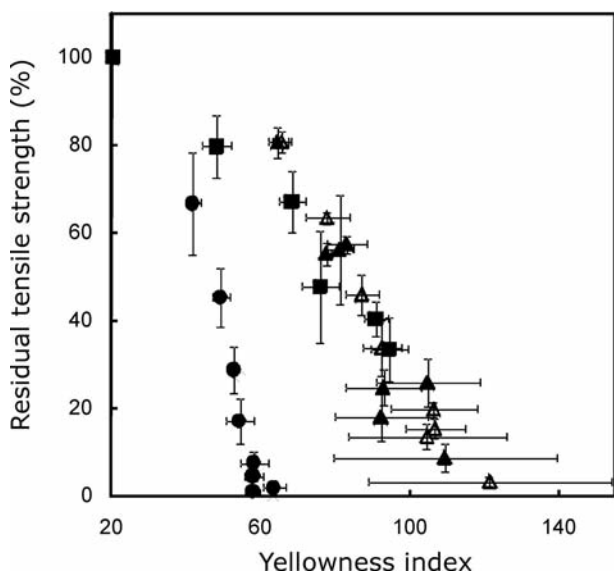


Figure 3. The correlation plots for % residual tensile strengths and yellowness indices of the artificially aged silks (symbols as for Figure 1); bars show the standard experimental errors. While the data points for the dry thermally aged and heat and humidity aged specimens seem to be similarly correlated, the data for the sunlight equivalent aged silk is quite distinct.

Plots of % residual tensile strengths of the silks against their yellowness indices (Figure 3) suggest a correlation, but indicate that light ageing is distinct, while dry thermal and oxic and anoxic heat and humidity aged specimens might be considered together.

Best fits to the time course data were determined with MS Excel, making the conservative assumption of a first order reaction with the first order rate constants determined from the tensile test results, while allowing variation of  $YI(\infty)$ . The consequent  $R^2$  values were 0.98, 0.74 and 0.96 for the dry thermal, combined heat and humidity, and sunlight equivalent ageing data respectively. The relatively poor fit for the combined heat and humidity data reflects the scattered nature of these points, which also showed large experimental errors at intermediate and longer ageing times. Nonetheless, the  $YI(\infty)$  values,  $125 \pm 10$  (dry thermal),  $115 \pm 5$  (heat and humidity),  $60 \pm 1$  (sunlight equivalent), are all consistent with the limits suggested in the correlation plots (Figure 3).

Silk fibroin is a semi-crystalline protein.<sup>9</sup> The yellowing of silk consequent upon sunlight irradiation (including the UV component) has been attributed to the oxidation of tyrosine, and further modification of intracrystalline amino acid residues.<sup>10</sup> The quite different change in yellowness effected by heat and humidity indicates a distinct cause for this discolouration. In these latter cases fibroin deterioration most likely predominates in the more accessible intercrystalline zones.<sup>4,9</sup> The deepening colour is reminiscent of that produced by the Maillard reaction in foodstuffs, in which amino acids combine with reduced sugars.<sup>11</sup> This proceeds at a faster rate as RH increases (although it slows at very high levels) and is also accelerated by heat. Fibroin has been reported to contain a small proportion of glucosamine (0.16%) and mannose (0.17%), both of which are reducing sugars<sup>12</sup>. The amino groups generated upon fibroin chain cleavage may then react to form N-glycosides, which after Amadori rearrangement to ketosamines, generate yellow-brown polymeric chromophores, offering a possible explanation for the colour changes observed. A similar explanation has been offered for the dark discolouration of gelatine-sized paper, when amino groups generated by gelatine proteolysis react with cellulose.<sup>13</sup> Others, though, have suggested that more extensive changes in the fibroin aminoacids (asp, glu, ser, thr followed by met, lys, arg, gly) alone account for the yellowing upon moist thermal ageing.<sup>14</sup> Further spectroscopic and mass spectrometric studies may provide clarification.

### 3.3 High Performance Size Exclusion Chromatography

Detailed analysis of the silk fibroin amino acid sequence, derived from the gene sequence, has shown that the protein is composed of a light (26 kDa) and a heavy (391 kDa) chain; these are covalently linked through a disulfide bond.<sup>15</sup> Unaged silk fibroin elutes as a well defined, relatively narrow peak in the chromatogram at 7.5 min (Figure 4), with an accompanying small satellite peak at 9.5 min (perhaps separated light chain). Upon initial degradation the main peak generally becomes skewed towards longer retention times. Subsequently, with further deterioration, other lower molecular weight peaks become evident, and these progressively gain in intensity. The fragmentation pattern of fibroin attests to the semi-crystalline nature of the heavy chain, with cleavage preferentially occurring within the amorphous regions between the crystallites.

Considering the variety of parameters that can be extracted from such chromatograms, the weight-averaged molecular weight ( $M_w$ ) has been reported to correlate best with the tensile strength of polymeric materials.<sup>16</sup> Since subtraction of the thiocyanate peaks from the chromatograms and reanalysis was not straightforward,  $M_w$  values were calculated for a slightly restricted silk envelope, integrating over the chromatographic traces between elution times of 6 and 12.5 min, ie nominally 2000 to 8 kDa from extrapolation of the calibration curve (Figure 4). This avoids inclusion of

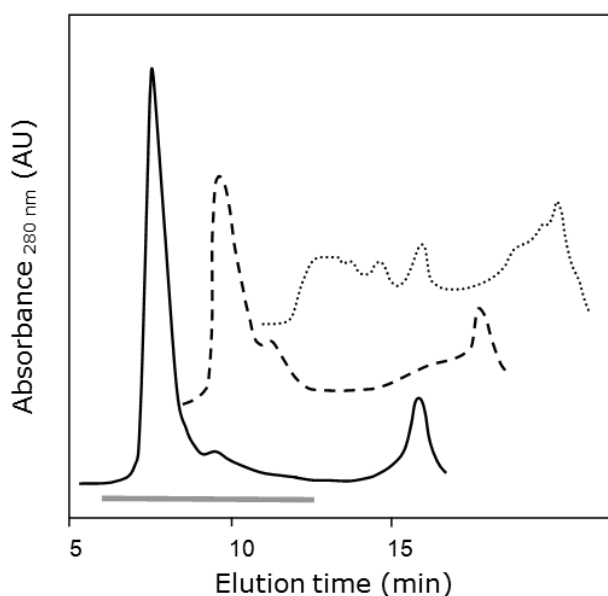


Figure 4. HPSEC chromatograms for unaged (solid line) and sunlight equivalent aged silk (8 days – dashed line, 20 days – dotted line); the traces are offset and shifted for ease of visualisation. Thiocyanate, the marker of the void volume, elutes at 16 min. The gray bar denotes that portion of a trace used for the weight-averaged molecular weight calculation. The chromatograms are typical of the variety of silk specimens.

the thiocyanate peak, but also leads to exclusion of small fibroin fragments. However, the consequent error in  $M_w$  is only significant for specimens subjected to extreme ageing, when fragmentation is severe. Plots of the calculated fibroin  $M_w$  over the three ageing time courses are presented in Figure 5.

The best fits to the time course data were determined, as for the yellowness indices, in this case allowing variation of  $M_w(\infty)$ . For the fits, the coefficients of determination were 0.98, 0.92 and

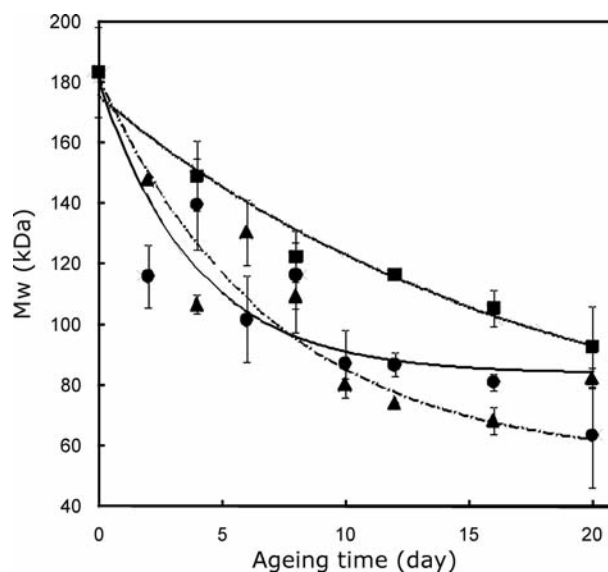


Figure 5. Plots of the change in fibroin HPSEC-derived weight-averaged molecular weights ( $M_w$ ) for each ageing regime (symbols and line styles as for Figure 1); bars show the standard experimental errors. The curves are best fits to the data, using the first order rates determined from the tensile test results.

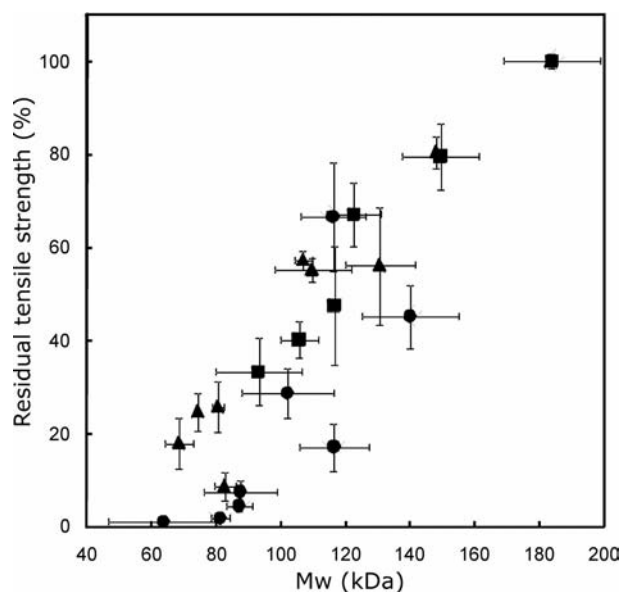


Figure 6. Correlation plots for the % residual tensile strengths and the fibroin weight-averaged molecular weights ( $M_w$ ) of the artificially aged silks (symbols as for Figure 1); bars show the standard experimental errors.

0.68 for the dry thermal, combined heat and humidity, and sunlight equivalent ageing data respectively. There was larger experimental error in the earlier time points for this last case. While the deterioration reactions may become rather complex, especially for highly degraded material, nonetheless, first order decay again seems to adequately describe the experimental data. The consequent values of  $M_w(\infty)$ ,  $55 \pm 5$  kDa (dry thermal, heat and humidity) and  $85 \pm 10$  kDa (sunlight equivalent), emphasise the differential effect of sunlight equivalent ageing. This would tie in with light (and especially UV) promoted chain rupture being followed by radical recombination, resulting in some cross-linking; photo-activated tyrosine residues, for example, will readily react with each other and with lysine.<sup>9</sup>

Once again there is a correlation between the measured parameter, the progressive reduction in  $M_w$ , and the decreased performance (Figure 6). Although the data points for sunlight equivalent ageing appear somewhat displaced from those for thermal and heat and humidity ageing, consistent with an extrapolation to a higher value for  $M_w(\infty)$ , the experimental error is such that statistical analysis does not differentiate the trends.

### 3.4 NIR spectroscopy – sorbed moisture

Unaged and aged silks exhibit only subtle differences in their NIR spectra. Nonetheless, we have demonstrated previously that an NIR spectrally-derived sorbed moisture parameter may have potential for distinguishing deteriorated fabrics.<sup>8</sup> This parameter is the normalized intensity of the moisture-related O-H combination band at  $5170 \text{ cm}^{-1}$  (Figure 7).

While there is some scatter in the data, the NIR spectral sorbed moisture parameter,  $I(5170)$ , shows a progressive decline during the three ageing experiments (Figure 8). Thermal ageing appears to induce the most pronounced effect, with sunlight equivalent ageing producing a much smaller change. The overlaid curves in Figure 8 show the best fits to the data points, generated as above while the  $I(5170)$  values at infinite time were allowed to vary. The associated  $R^2$  values (0.94, 0.62 and 0.27) highlight the increased scatter from thermal, through high heat and humidity to sunlight equivalent ageing, rather than suggesting a need to consider a higher order reaction. The limiting  $I(5170)$  values ( $1.2 \pm 0.1$ ,  $2.2 \pm 0.1$ ,  $2.5 \pm 0.1$ ) once again match those anticipated from the correlation

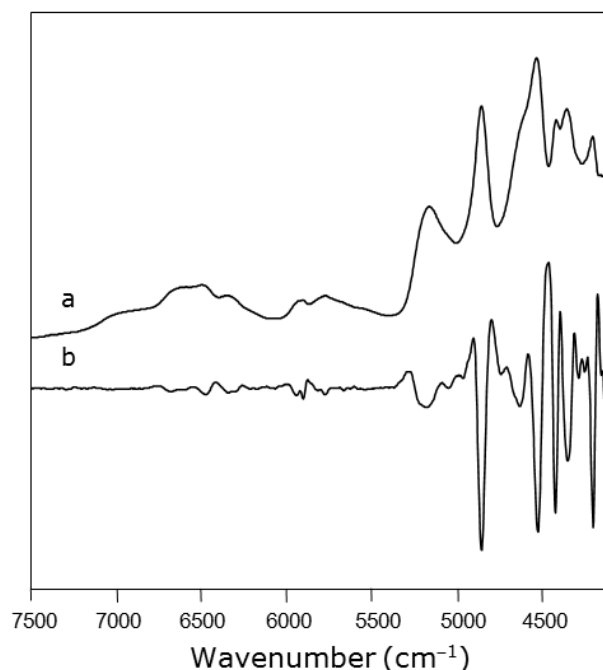


Figure 7. a) The NIR absorbance spectrum of a sample of silk aged under sunlight equivalent conditions for 10 days, over the spectral range which shows the major bands, and b) the second derivative function of the Kubelka Munk corrected spectrum. The features of interest for the sorbed moisture analysis are the O-H combination band at  $5170 \text{ cm}^{-1}$  and the methylene overtone band at  $5944 \text{ cm}^{-1}$ .

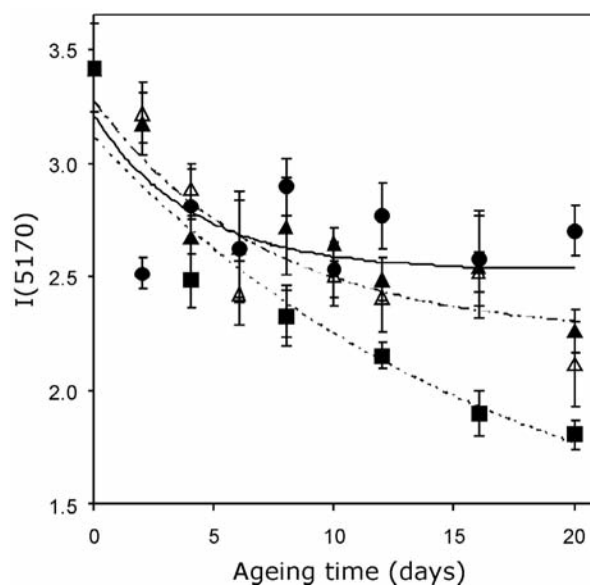


Figure 8. Illustrations of the changes in the NIR spectral sorbed moisture parameter,  $I(5170)$ , upon the gradual deterioration of silk under the three different ageing regimes. The symbols and line styles are as in Figure 1, and bars show the standard experimental errors. The curves are best fits to the data, using the first order rates determined from the tensile test results.

plots (Figure 9), lending some confidence to the analysis.

The % residual tensile strengths versus  $I(5170)$  plots (Figure 9) suggest somewhat different trends for the three ageing conditions. While there are good correlations for the separate thermal and high heat and humidity aged silk data sets, the

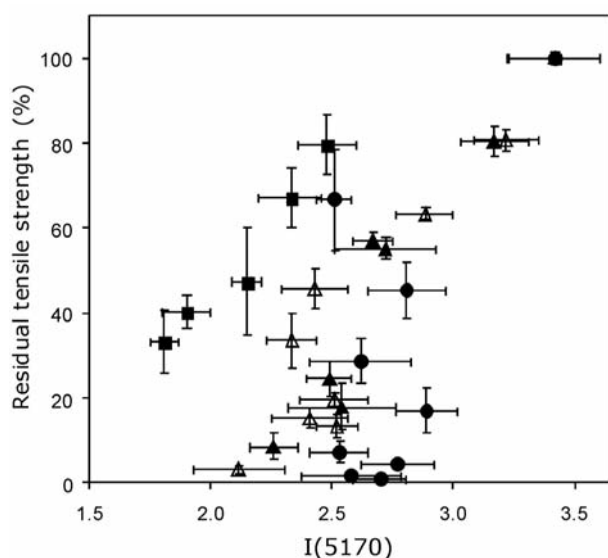


Figure 9. Correlation plots for the % residual tensile strengths and I(5170), the NIR spectral sorbed moisture parameters of the artificially aged silks (symbols as for Figure 1); bars show the standard experimental errors.

data points for the sunlight equivalent aged material show a relatively large experimental error and significant scatter.

The general reduction in moisture sorption following ageing must result principally from changes to the intercrystalline amorphous regions of silk fibroin. Here, for an RH of 50% and unaged material, structural and bound water is present, at a level of around 7% by weight of silk.<sup>8</sup> The bound water helps to maintain the plasticity of the amorphous zones by keeping chain segments apart. During dry thermal ageing there will be significant desiccation. As a consequence, increased intra- and inter-chain secondary bonding will occur, promoted by peptide cleavage which will allow increased chain mobility. The resulting deteriorated silk will absorb moisture far less readily; a limiting 60% reduction is seen. In contrast, ageing at high temperature and high humidity should restrict any rearrangement of the disordered regions, as the interactions with sorbed moisture are retained. Such aged silks will then exhibit a smaller reduction in moisture content, relative to unaged material, when subsequently equilibrated at 50% RH; experimentally the decrease is just one third. Further analysis of the NIR spectra lends support to this interpretation, which infers some ordering of the amorphous segments. The band at 4640  $\text{cm}^{-1}$ , attributed to an amide combination mode for the amorphous region, remains at similar intensity throughout the high heat and humidity ageing time course, but diminishes by around one fifth during dry thermal ageing. Extended sunlight equivalent ageing at intermediate RH effects a drop in the moisture sorption of just 25%, suggesting that new

inter-fibroin secondary bonding may again be constrained, although chain mobility following photo-induced cleavage will ensure some such interactions.

#### 4 Conclusions

Previously we have suggested that the condition of silk was affected by fibroin chain cleavage in the amorphous zones, and that analytical techniques which could directly or indirectly report on these events might permit condition monitoring. In the research reported here, which again indicates first order fibroin decay, correlations are observed between the tenacity of the artificially aged silks and their yellowness indices, HPSEC-derived weight-averaged molecular weights and NIR spectral moisture sorption parameters. In appropriate circumstances, all three associated techniques could be used to assess the physical condition of silk, to inform conservation and display.

For dry thermal and heat and humidity aged material (under oxic and anoxic conditions), the yellowness index may allow a simple measure of the generation of amine groups following chain cleavage. While the correlation for sunlight equivalent ageing is different, nonetheless, the yellowness index appears to relate to the photo-induced fibroin cleavage and further oxidation of amino acid residues. Two separate models are necessary for the correlation of the yellowness indices and silk condition (eg tenacity).

HPSEC provides a direct measure of fibroin disruption, in terms of the weight-averaged molecular weight. While we and others have previously used HPSEC to gauge condition,<sup>3,6,9</sup> the present detailed results suggest that separate correlation models may be required for silks exposed to different effectors of deterioration. In particular, silk fibroin which has been exposed to sunlight with a UV component may become cross-linked, and hence exhibit unique behaviour.

Moisture sorption by aged silk is also dependent on the history of exposure, with the various effectors of deterioration eliciting different responses.

This research forms part of a wider programme with the overall aim of developing rapid and routine, non-invasive near infrared methodology for characterising the physical condition of silks in collections. The outcomes of the present work suggest the need for caution when developing the associated predictive chemometric model. Silks subjected to the variety of degradative causes must be incorporated in the reference set if an all encompassing model is to be attained.

## 5 Acknowledgements

This research was completed while JK was a Research Fellow in the AHRC Research Centre for Textile Conservation and Textile Studies, at the Textile Conservation Centre. She was supported by the Korean Research Foundation Grant funded by the Korean Government(MOEHRD), KRF-2006-214-C00104. We are indebted to Maria Hayward, Director of the Research Centre, and Nell Hoare, Director of the TCC. The work would not have been possible without the support of all our colleagues at the TCC, especially Paul Garside and Naomi Luxford.

## 6 References

1. P. Garside, P. Wyeth, *Characterization of historic silk by polarized attenuated total reflectance Fourier transform infrared spectroscopy for informed conservation*, Appl. Spectrosc., 2005, **59**, 1242-1247.
2. J. Kim, X. Zhang, P. Wyeth, *The inherent acidic characteristics of aged silk*, e-Preserv. Sci., 2008, **5**, 41-46.
3. K. Hallett, D. Howell, *Size exclusion chromatography as a tool for monitoring silk degradation in historic tapestries*, in: R. Janaway, P. Wyeth, Eds., *First annual conference of the AHRC Research Centre for Textile Conservation and Textile Studies, Scientific Analysis of Ancient and Historic Textiles: Informing Preservation, Display and Interpretation*, Winchester, 13-15 July 2004, Archetype Publications, London, 2005, 143-150.
4. M.A. Becker, Y. Magoshi, T. Sakai, N.C. Tuross, *Chemical and physical properties of old silk fabrics*, Stud. Conserv., 1997, **42**, 27-37.
5. E. Richardson, G. Martin, P. Wyeth, X. Zhang, *State of the art: Non-invasive interrogation of textiles in museum collections*, Microchim. Acta, 2007, **162**, 303-312.
6. K. Hallett, D. Howell, *Size exclusion chromatography of silk: inferring the textile strength and assessing the condition of historic tapestries*, in: I. Verger, Ed., *Preprints 14th ICOM-CC Triennial Meeting*, The Hague, 12-16 September 2005, James and James, London, 2005, 911-919.
7. J. Bello, *Heat capacity and volume changes of protein denaturation*, J. Phys. Chem, 1978, **82**, 1607-1609.
8. X. Zhang, P. Wyeth, *Moisture sorption as a potential condition marker for historic silks: Noninvasive determination by near-infrared spectroscopy*, Appl. Spectrosc., 2007, **61**, 218-222.
9. P. Garside, P. Wyeth, *Chp. 4 Textiles*, in: E. May, M. Jones, Eds., *Conservation Science: Heritage Materials*, Royal Society of Chemistry, Cambridge 2006, 56-91.
10. J. Shao, J. Zheng, J. Liu, C.M. Carr, *Fourier transform Raman and Fourier transform infrared spectroscopy studies of silk fibroin*, J. Appl. Polym. Sci., 2005, **96**, 1999-2004.
11. F. Ledl, E. Schleicher, *New aspects of the Maillard reaction in foods and in the human body*, Angew. Chem., 1990, **29**, 565-594.
12. P. Calvini, A. Gorassini, *FTIR-deconvolution spectra of paper documents*, Restaurator, 2002, **23**, 48-66.
13. S. Hyogo, A. Yoshiko, *Carbohydrate content of fibroin and sericin of the silkworm, Bombyx mori*, J. Biochem., 1967, **62**, 129-130.
14. K. Setoyama, *Effect of water on the heat-yellowing of silk fabric and the change in amino acid composition in the silk fibroin in the sealed tubes by heat-treatment*, J. Sericult. Sci. Japan, 1982, **51**, 365-369.
15. C.-Z. Zhou, F. Confalonieri, M. Jacquet, R. Perasso, Z.-G. Li, J. Janin, *Silk fibroin: Structural implications of a remarkable amino acid sequence*, Prot.: Struct., Funct. Gen., 2001, **44**, 119-122.
16. A.B Mathur, I.S. Bhardwaj, *Chp. 19 Performance of polyethylenes in relation to their molecular structure*, in: N. P. Cheremisinoff, Ed., *Handbook of engineering polymeric materials*, Marcel Dekker, New York, 1997, 277-294.